

Article

Real-Time Methane Prediction in Underground Longwall Coal Mining Using AI

Doga Cagdas Demirkan ^{1,*}, H. Sebnem Duzgun ^{1,*}, Aditya Juganda ¹, Jurgen Brune ¹ and Gregory Bogin ²

¹ Mining and Earth Systems Engineering Program, Mining Engineering Department, Colorado School of Mines, Golden, CO 80401, USA

² Mechanical Engineering Department, Colorado School of Mines, Golden, CO 80401, USA

* Correspondence: demirkan@mines.edu (D.C.D.); duzgun@mines.edu (H.S.D.)

Abstract: Detecting the formation of explosive methane–air mixtures in a longwall face is still a challenging task. Even though atmospheric monitoring systems and computational fluid dynamics modeling are utilized to inspect methane concentrations, they are not sufficient as a warning system in critical regions, such as near cutting drums, in real-time. The long short-term memory algorithm has been established to predict and manage explosive gas zones in longwall mining operations before explosions happen. This paper introduces a novel methodology with an artificial intelligence algorithm, namely, modified long short-term memory, to detect the formation of explosive methane–air mixtures in the longwall face and identify possible explosive gas accumulations prior to them becoming hazards. The algorithm was trained and tested based on CFD model outputs for six locations of the shearer for similar locations and operational conditions of the cutting machine. Results show that the algorithm can predict explosive gas zones in 3D with overall accuracies ranging from 87.9% to 92.4% for different settings; output predictions took two minutes after measurement data were fed into the algorithm. It was found that faster and more prominent coverage of accurate real-time explosive gas accumulation predictions are possible using the proposed algorithm compared to computational fluid dynamics and atmospheric monitoring systems.



Citation: Demirkan, D.C.; Duzgun, H.S.; Juganda, A.; Brune, J.; Bogin, G. Real-Time Methane Prediction in Underground Longwall Coal Mining Using AI. *Energies* **2022**, *15*, 6486. <https://doi.org/10.3390/en15176486>

Academic Editor: Krzysztof Skrzypkowski

Received: 3 August 2022

Accepted: 1 September 2022

Published: 5 September 2022

Publisher's Note: MDPI stays neutral with regard to jurisdictional claims in published maps and institutional affiliations.



Copyright: © 2022 by the authors. Licensee MDPI, Basel, Switzerland. This article is an open access article distributed under the terms and conditions of the Creative Commons Attribution (CC BY) license (<https://creativecommons.org/licenses/by/4.0/>).

Keywords: artificial intelligence (AI); computational fluid dynamics (CFD); underground coal mines; methane prediction; real-time; time series prediction; modified long short-term memory

1. Introduction

Despite alternative energy sources, worldwide coal production is still increasing each year [1]. Longwall mining is the most utilized coal mining method, due to its high productivity and safer operating conditions [2]. However, in usual mining operations and conditions, coal mining still faces serious challenges [3]. Despite advancements in technology and safety management, longwall face explosions from accumulated methane gas are known to be the most common causes of methane explosions [4]. Existing industry practices depend on point-type methane sensors in critical regions to prevent explosive gas accumulations [5]. However, point sensors are not reliable at spotting and warning about explosion hazards, especially in crucial areas, such as near the cutting drum, tailgate, and headgate areas of the longwall face [6]. One catastrophic example of a methane explosion accident was the 2010 Upper Big Branch Mine in West Virginia, U.S. [6]. Although atmospheric monitoring systems can report real-time methane concentrations, they fall behind due to their limited number of sensors and locations [7], which lack full coverage of the whole longwall face. Computational fluid dynamics (CFD) were employed to simulate ventilation conditions in longwall faces to reproduce airflow aerodynamics and the formation of hazardous gas mixtures which are not detectable using conventional monitoring and ventilation inspection practices [5]. Although CFD modeling can accurately predict explosive gas zones, high computational power and time requirements render its use for real-time ventilation monitoring purposes impossible [7].

Karacan (2008) proposed principle component analysis and an artificial neural network-based approach to predict methane emission rate throughout 63 longwall mines. The study shows that the volume of daily methane emission from each mine can be accurately predicted [8]. Dougherty and Karacan (2011) utilized the prediction model in [8] and developed software which can predict ventilation emissions with elastic properties [9]. Duda and Krzemień (2018) proposed a framework for forecasting methane emissions from seams to goafs; they predicted the average volume of methane per minute in each year of mine life [10]. Sidorenko et al. (2021) provided the necessary parameters to predict methane emissions from seams to goafs [11]. Although these studies discuss prediction, these predictions are neither real-time nor spatial outputs.

Previous studies demonstrate the successful implementation of Artificial Intelligence (AI) in various fields with real-time predictions. For example, Chen et al. (2019) proposed a real-time AI integration for cancer diagnosis by implementing image processing algorithms for body scans [12]. Nyanteh et al. (2013) implemented an AI for real-time fault detection [13]. To improve weather forecasting for high-impact weather, McGovern et al. (2017) integrated an AI with expert opinions [14]. Imran et al. (2014) classified real-time messages in social media using AI to help the public access important disaster response information [15]. Dong et al. (2021) used the AI model for real-time monitoring and predicting of slope failures [16]. Rodríguez-Rangel et al. (2022) incorporated big data analytics for autonomous vehicles' speed estimation [17]. Wahyono et al. (2022) proposed combining AI with data mining for real-time forest fire detection [18].

Real-time prediction of methane in a longwall face requires predicting explosive gas zone formation in time, and its location in 3D (x , y , and z coordinates). Predictions in time are mainly conducted using time series classification/analysis [19]. Spatiotemporal AI models and time series classification are relatively new to the field. Moreover, the vast majority of successful models only take into account one or two spatial dimensions, such as x and/or y coordinates, and the data of interest [20–28]. For example, whereas climate change studies that track carbon emissions use latitude, longitude, and carbon content [29], water quality studies use one-dimensional distance of the intersections and water content [19]. This study proposes a 3D spatiotemporal prediction model for the real-time prediction of methane in the coal face.

Current explosive gas accumulation monitoring practices in longwall coal mines rely on two methods, namely, point sensors and CFD modeling. Point sensors take real-time measurements along the face and provide methane concentration values at the installed locations. CFD modeling provides methane prediction for the whole longwall face. However, due to computational cost, predictions take days or weeks, depending on the resolution of the study area. In this study, a continuation of our previous work [7] benchmarking and analyzing the suitability of the dataset and off-the-shelf algorithms, we developed an AI algorithm and methodology for use as a real-time explosion hazard warning system. We used six CFD analyses with varying shearer locations to train, test, and validate our model. This approach lays the foundation for accurate methane predictions in real-time for underground mines by combining the most potent advantages of point sensors and CFD models, decreasing the computational cost of CFD modeling, and increasing the coverage of point sensors.

Previously conducted methane prediction studies mainly focused on total methane emissions from the seam or the whole mine. To the best of our knowledge, a 3D real-time methane prediction approach in longwall mining that integrates CFD data with an AI model has not been developed yet. Previous studies of methane prediction in longwall coal mines primarily focused on total methane emissions of the whole mine or the whole face with varying time intervals of years to minutes. Moreover, the predictions in these studies do not consider critical methane emission zones, such as near the drums or shearer locations. This paper fills these gaps. The approach presented herein can provide methane emission data not only in the 3D spatial domain but also in real-time throughout the mining

face, including, but not limited to, areas near cutting drums, the shearer, the tailgate, and the headgate.

The remainder of this paper is organized as follows. Section 2 describes materials and methods used in this study. Section 3 describes empirical results from the AI model. Section 4 discusses and compares results. Lastly, Section 5 summarizes the paper, makes concluding remarks, and outlines future work.

2. Materials and Methods

The developed research methodology exploits the advantages of CFD modeling and point sensors. Figure 1 illustrates how AI was integrated into real-time methane concentration prediction.

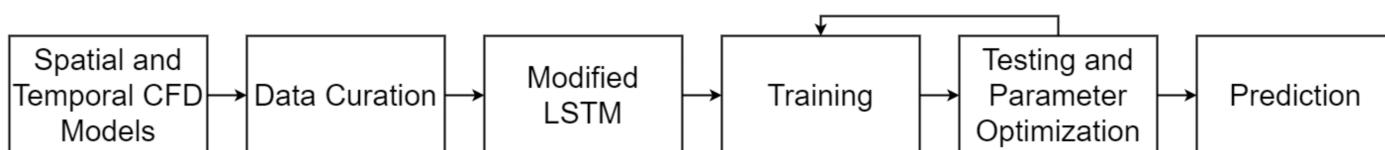


Figure 1. Research methodology.

The first step explains spatial and temporal CFD modeling and longwall face simulation. The second step presents extracted data and how they were processed and presented. The third step discusses an AI algorithm, referred to as the long short-term memory (LSTM) model, and how it was modified to meet this study's requirements; the algorithm was trained and tested, and parameters were optimized. In the last step, predictions for spatial and temporal results are discussed.

2.1. Spatial and Temporal CFD Modeling

Ansys Fluent software version 18.2 was utilized to model and simulate a longwall face. The modeled longwall face was 300 m long with a mining height of 3 m and a depth of 6 m. Two primary pieces of equipment were also modeled: (i) support equipment (shields) and (ii) cutting equipment (shearers). There were 150 shields; each shield was 2 m long, fixed in the model. One 10 m long shearer was placed along the longwall face in 6 locations. Location details are provided in Section 2.2. Lastly, the modeled area was covered with approximately 31 million hexagonal and octagonal meshes. Mesh sizes ranged from 3 cm to 30 cm, which increased prediction resolution.

The simulation exemplified a transient CFD model of methane (CH₄) gas emission from the coal face based on a bleeder ventilation system with a tailgate (TG) back return setup. Each transient model was simulated for 180 s and recorded at 1 s intervals.

2.2. Data Curation

Data were collected after modeling the longwall and simulating methane emissions. It should be noted that although each mine ventilation condition is unique, previously conducted studies [30–34] validate that simulated data are consistent with the actual situation that includes but is not limited to “(i) continuous leakage of fresh air from the face to the gob, and the higher accumulation of methane as the supplied air travels from the headgate to tailgate side of the face; (ii) higher leakage around the headgate and tailgate corners of the face due to the high porosity and permeability around the edge of the gob; (iii) Methane accumulation seems to follow linear regression based on ventilation surveys done in several longwall operations.” [4].

Each simulation had approximately 31 million cells; data for each cell for each second of recording included pressure, airflow velocity (V_x, V_y, and V_z), CH₄ concentration, cell volume, and x, y, and z coordinates. Data collection was repeated for each of the shearer's six locations, which required 10 days for each location. Details of specific shearer locations and the cutting direction during data collection are provided in Figure 2.

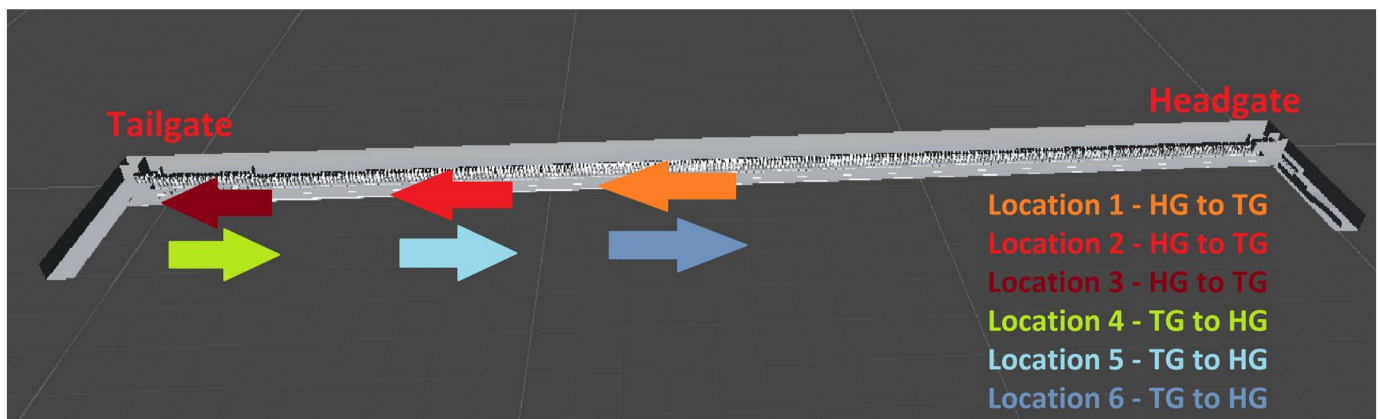


Figure 2. Six locations of the shearer and cutting directions during data collection.

Figure 3 represents a snapshot of the 120th second of location 3 as an example. Other locations and timestamps acted similarly; to avoid redundancy only one example is provided.

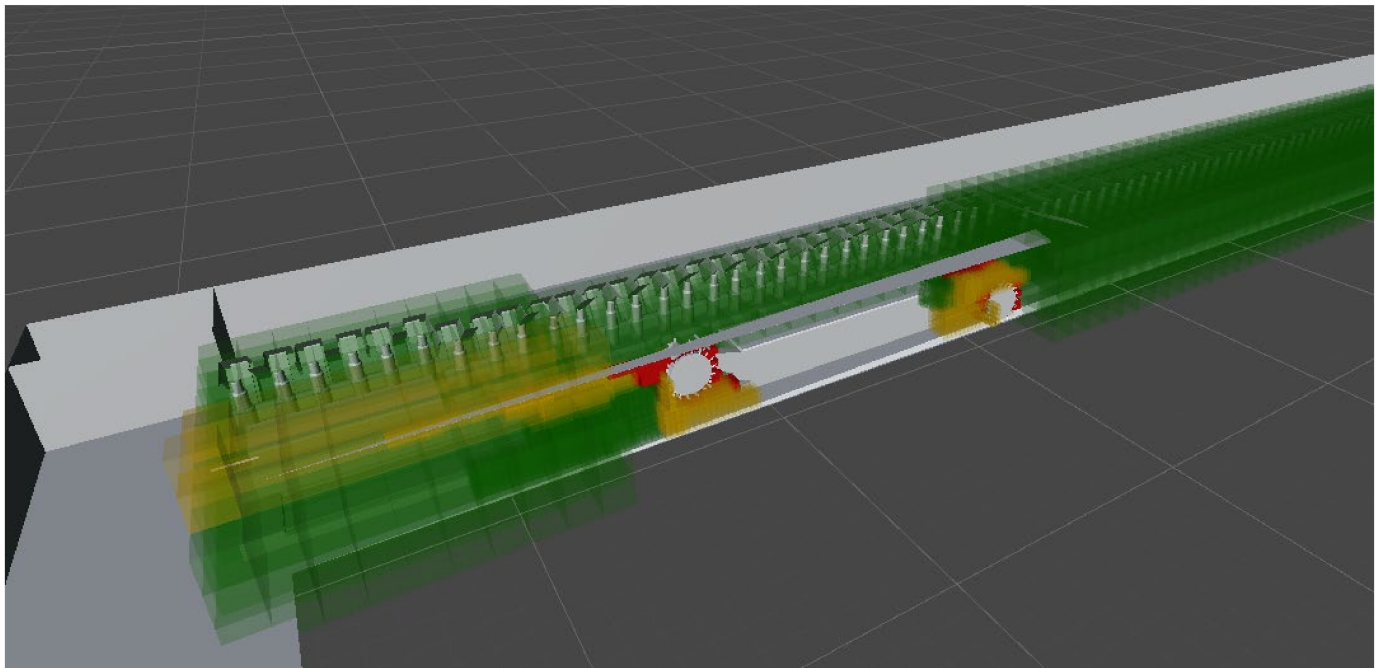


Figure 3. Snapshot of the 120th second of shearer location 3.

Raw data from the Fluent software were preprocessed, which included data conversion into CSV files, removing empty fields, adding cutting directions, and fixing the two significant figures for all fields. There were 2 terabytes (TBs) of end data for each location; 12 TBs of data were input into the AI.

2.3. The Modified LSTM

The literature discusses different methods for the spatiotemporal prediction of a parameter, namely, the Naïve 2 method, simple exponential smoothing, the Holt method, the ARIMA method, and the ETS method [35]. The primary disadvantage of using the Naïve 2, simple exponential smoothing, and HOLT methods is that these algorithms can only predict one step ahead of time within a confidence interval. In a dynamic environment such as longwall mining, continuous monitoring is the key to preventing explosive hazards; hence, one-step-ahead predictions were not sufficient for the aim of this study. Moreover, it was not feasible to implement these methods for real-time prediction considering the

required computational power and data size. For example, each location had approximately 32 million cells, which were connected to each other and affected methane concentration. In contrast, the ARIMA and ETS methods can predict long-term methane concentrations for a specific cell. However, the longwall's geometry was 3D, and these statistical methods are not effective at predicting in a 3D environment. Moreover, unlike AI models, statistical methods utilize interpolation that cannot learn data's extreme fluctuations.

AI and machine learning (ML) algorithms have been recently introduced to predict the time and location of a parameter of interest. Although applications are still limited, preliminary results of a range of studies (discussed briefly in Section 1) are promising. Moreover, in-depth analysis and benchmarking of the most promising algorithms for real-time methane prediction were examined in a previous study [7].

In light of the literature and previous tests, a recurrent neural network (RNN) was determined to be the best candidate for real-time methane prediction in longwall coal mines. An RNN contains cycles from previous time steps as network inputs to influence predictions at the current time step. These timestamps are stored in the RNN's internal states, allowing it to exploit a dynamically changing contextual window over the input sequence history [36–38].

Unfortunately, the range of contextual information that a standard RNN can access is, in practice, quite limited. The problem is that the influence of a given input on the hidden layer and, therefore, on the network output, either decays or blows up exponentially as it cycles around the network's recurrent connections. This shortcoming is referred to in the literature as the vanishing gradient problem. Long short-term memory (LSTM) is an RNN architecture specifically designed to address the vanishing gradient problem [39–41]. LSTMs were introduced in about 1997; their main advantages include that they are (i) algorithms that can store information for a specified time duration, (ii) resistant to noise, and (iii) trainable parameters [42,43]. In the light of our previous study [7], any future prediction using AI can be categorized into seven problem types (image, sensor, motion, spectrographs, electronic devices, electrocardiograms, and simulations). As methane prediction is similar to the sensor-type problem, one of the best performing algorithms, an LSTM network (a special type of RNN) was adapted for this study.

Figure 4 shows the simplified architecture of the LSTM model, modified from the blog post by Olah [37]. In the forget gate, the cell takes the previous time step and determines which information should be kept and which should be omitted. In the input gate, the cell takes information and keeps only what is relevant for prediction. In the update gate, the cell takes previous neural network information and updates prediction weights. Lastly, the output gate determines which parameters and data to output and feed to the next cell.

As LSTMs are viewed as feed-forward neural networks where each cell shares the same model parameters, they are considered deep architectures or deep neural networks [36]. In this study, the LSTM network was modified, trained, and tested with CFD outputs. A conventional LSTM network accepts 2D data. LSTM model modifications implemented in this study include (i) changing the input shape for the 3D space and (ii) adding 3D operations and vector calculations. The inputs to the modified LSTM model were; x , y , and z coordinates, the smallest distance to the shearer, airflow velocity, methane concentration, and the volume of each cell for 180 s, which were recorded at 1 s intervals.

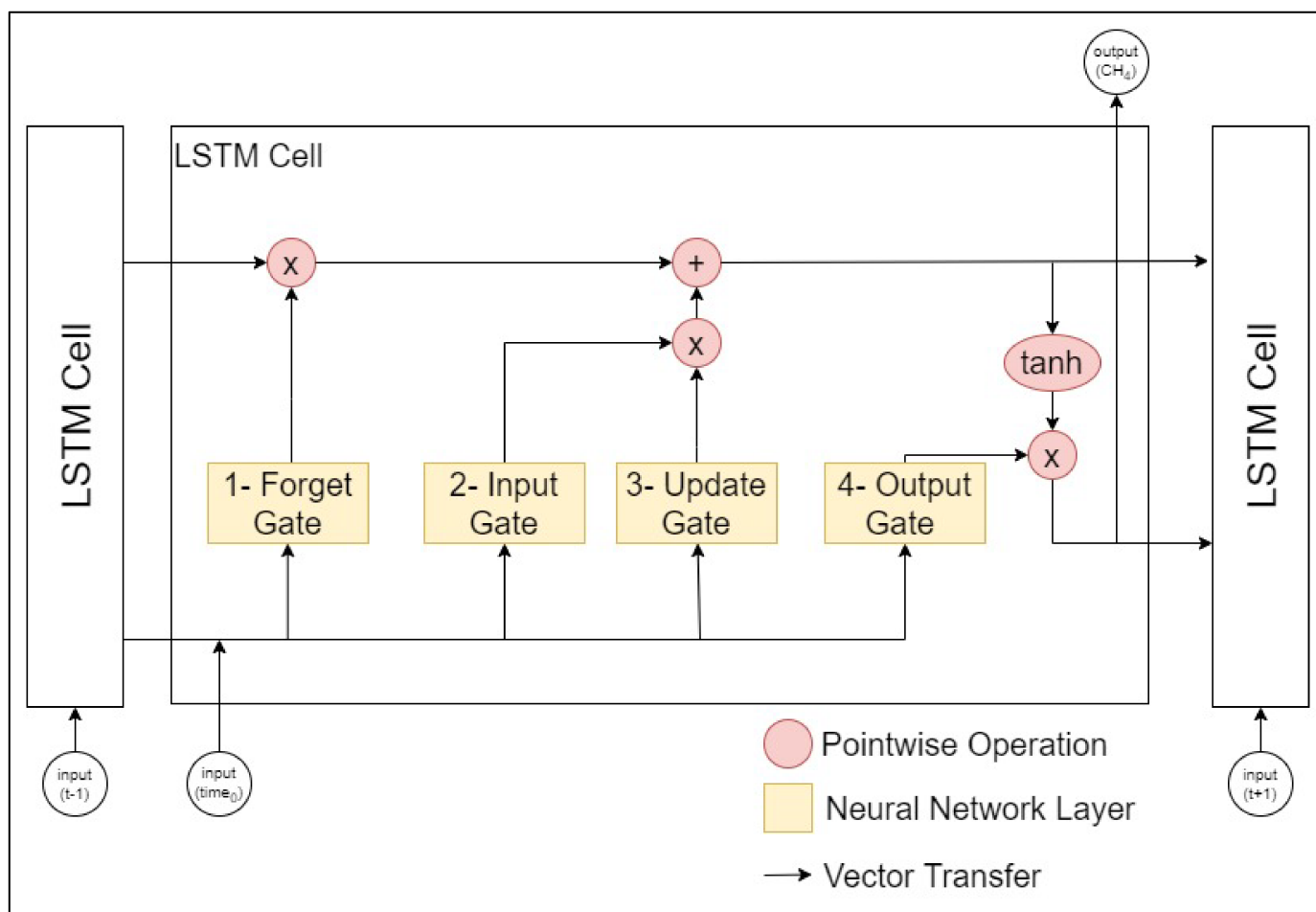


Figure 4. Simplified LSTM architecture (modified from [37]).

3. Results

Even the best-performing algorithms might fail to predict results without high-quality data. Therefore, training, validation, and testing of the algorithm are critical for reliable predictions; if these steps are not performed correctly results might be biased. Table 1 provides a data breakdown, and is followed by an explanation of each topic in respective subsections. Note that similar shearer locations were selected for training and predicting methane content. For example, Figure 2 illustrates that shearer locations 1 and 6 had a similar location in the middle of the longwall face, and locations 3 and 4 had a similar location on the tailgate side. In addition to slight changes in the exact positions of cutting equipment, cutting directions were also changed. Datasets for similar locations were divided 50–50 for training and testing. The first 50% was divided into 80% to 20% for training and validation; the detailed distribution is provided in Table 1.

Table 1. Training, validation, and testing datasets based on shearer locations.

Training DataSet	Validation DataSet	Cutting Direction	Testing DataSet	Cutting Direction
80% of Location 1	20% of Location 1	Headgate to Tailgate	Location 6	Tailgate to Headgate
80% of Location 2	20% of Location 2	Headgate to Tailgate	Location 5	Tailgate to Headgate
80% of Location 3	20% of Location 3	Headgate to Tailgate	Location 4	Tailgate to Headgate
80% of Location 4	20% of Location 4	Tailgate to Headgate	Location 3	Headgate to Tailgate
80% of Location 5	20% of Location 5	Tailgate to Headgate	Location 2	Headgate to Tailgate
80% of Location 6	20% of Location 6	Tailgate to Headgate	Location 1	Headgate to Tailgate

The common practice of splitting data into train, validation, and test sets depends on the dataset and might range from 50–50% to 80–20%. With a few data points ($n < 10,000$), 70–30% splitting is used. However, if the number of recordings is high ($n > 1,000,000$), the importance of split ratios decays. Overall, the most important element in splitting a dataset is having good data representation in the train and test sets. In this study, the number of recordings was close to 64,300,000; hence, training was conducted using a specific shearer direction and tested using the opposite direction but the same position [44–48].

The training and validation of each instance took approximately seven days; testing time was 15 min with high-performance computing using the following specifications:

- CPU: Intel Xeon COU E704830 v3@2.10GHz (4 CPUs/node, 48 cores/node)
- GPU: five Tesla K80
- Memory: 2133 MT/s, Dual Rank, x4 Data Width RDIMM (42.7 GB/Core)
- Storage: 20 TBs

Input data were approximately 5 TBs for each instance, with 2 TBs of output.

3.1. Training

Training data were used to teach patterns and features to the AI model. The same training data were repeatedly given to the model until a threshold level was reached. Feeding the same data repeatedly is called an epoch. The simple explanation of an epoch is one complete pass of the dataset through the designed network. The algorithm updated its parameters with each epoch while learning the input dataset. Training data were divided into 80% and 20% for each instance using the stratified K-folds cross-validation method. This yielded a balanced data division, which preserved the percentage of samples for each methane content. The divided 80% of data were used to train the model.

3.2. Validation

Validation data were separated from training data, which validated the AI's performance. Training and validation accuracy helps users evaluate their mode. Figure 5 illustrates a commonly used metric for assessing algorithm performance, validation, and training accuracy versus an epoch.

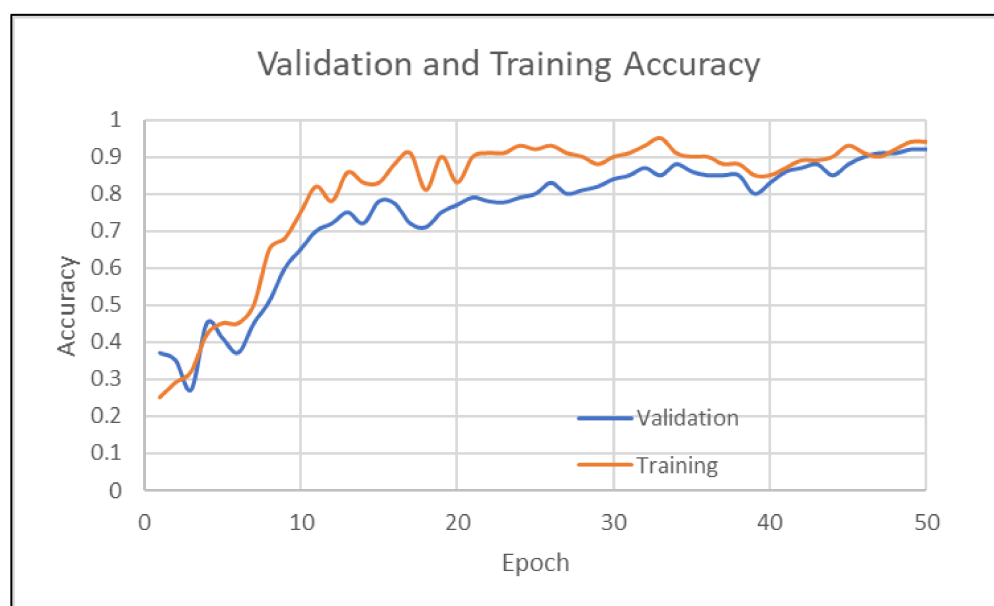


Figure 5. Validation and training accuracy.

In the training and validation accuracy graph, the curves' slopes approach horizontal after the 12th epoch, which indicates that data did not make a significant learning process over the algorithm. At approximately the 20th epoch, the learning curve becomes almost

horizontal. This indicates that no further training was necessary after the 20th epoch, as the accuracies did not change considerably and ranged from 89.1% to 93.8%. Lastly, the validation curve below the training curve indicates that the model was fed a good representation of data, was ready for testing, and able to provide reliable predictions.

3.3. Testing

After training and validation, test data were used to evaluate the AI model's performance predicting methane. The model's performance was analyzed using the actual and predicted methane content of the testing data for each training and testing coupled set, as provided in Table 2.

Table 2. Overall accuracies of tests.

Couple Name	Training DataSet	Testing DataSet	Overall Accuracy
L1L6	Location 1	Location 6	92.4%
L2L5	Location 2	Location 5	89.1%
L3L4	Location 3	Location 4	87.9%
L4L3	Location 4	Location 3	88.3%
L5L2	Location 5	Location 2	91.0%
L6L1	Location 6	Location 1	91.6%

These results show that the modified LSTM algorithm predicted methane concentration with an accuracy ranging from 87.9% to 92.4%.

4. Discussion

Analysis revealed that the modified LSTM algorithm can possibly combine effective aspects of CFD modeling and point sensor measurements. AI algorithms can achieve 3D coverage of CFD modeling and real-time point sensor data measurements. The overall accuracies of different locations ranged from 87.9% to 92.4%. Although accuracies were relatively high, some locations (such as locations 3 and 4) had less accurate results than others, possibly because the closer the shearer was to the headgate and tailgate (locations 1 and 6), the more methane emissions fluctuated. The algorithm was more agile when spotting fluctuations; therefore, relatively constant methane emissions might be the reason for lower test accuracies in locations 3 and 4. Although the accuracies showed promising results, with additional datasets they might increase. Even if a single location has approximately 32 million points, the entire measurement only contains 180 s of data. If these measurements could be increased, accuracies might also increase. Given the current data storage and computational power advancements in supercomputers, the required time for training was 45 days. Moreover, an increase in data size will increase the required computational power and time required for training; however, time requirements will change more exponentially than linearly. Training times will not affect prediction times; once the algorithm is trained, the required prediction time will not change drastically.

Whereas explosive gas zone monitoring relies on point sensors, the critical regions of the longwall face cannot be tracked in real time. Although CFD modeling can overcome the sensors' coverage, the required prediction time could be days to weeks, depending on the resolution of the simulation. This study's methodology eliminates these shortfalls. The system proposed herein yields highly accurate real-time predictions with detailed coverage of the longwall face. Therefore, modified LSTM-based methane prediction might help early warning systems for miners and engineers reduce safety risks and prevent accidents such as the Upper Big Branch. Lastly, the system can increase production by reducing unnecessary stops of the shearer.

However, the AI's prediction capabilities depend on the simulated CFD model results. Therefore, predictions can only be as accurate as similar longwall face models. Training

the AI model using different longwall face models can increase the AI model's capacity. If the AI model can be trained with more data, it might be used for all longwall mines in the world.

5. Conclusions

As was the case with the Upper Big Branch accident, longwall mine methane explosions can be fatal. Current explosive gas zone management practices are carried out either with point sensors or CFD modeling. Leveraging the power of AI might be crucial for monitoring explosive methane concentration. The primary objective of this study was to combine the advantages of current methane monitoring practices and eliminate their disadvantages. For this purpose, modified LSTM architecture was utilized for real-time methane prediction.

This study is unique as it provided real-time methane prediction in 3D space. Our study successfully leveraged a significant (12 TB) amount of CFD data for location and time prediction of possible explosive methane accumulation. Unnecessary stops, high fan speed, and other high operating costs can be reduced using the proposed method, which will help increase the safety and productivity of all longwall coal mines by monitoring the methane gas along the face.

Although the proposed methodology successfully predicted methane concentration throughout the longwall face, the results only contained numbers representing location, time, and methane content. Results consisted of lines of numbers that could not be interpreted or used by engineers and/or miners to determine if the explosive gas accumulation was hazardous.

Future research associated with this study will consist of two parts. First, the algorithm will be trained using other mines' methane emission models. This will increase the algorithm's prediction capabilities and enable its usage and implementation on all longwalls in the world. Second, the predictions of the AI model will be imported into Unity for visualization purposes. This will help facilitate the integration of real-time predictions with augmented and virtual reality environments, which are already implemented in other industries, such as construction, production, health, and many more. The final product might ease the judgement burden placed on engineers and workers in times of critical methane emission. We will convert results into more robust, understandable visualizations that resemble CFD output; providing a familiar output will help engineers and workers by decreasing their cognitive load.

We have started the second development phase; a side-by-side comparison of the CFD model and our visualizations for different time stamps are shown in Figure 6.

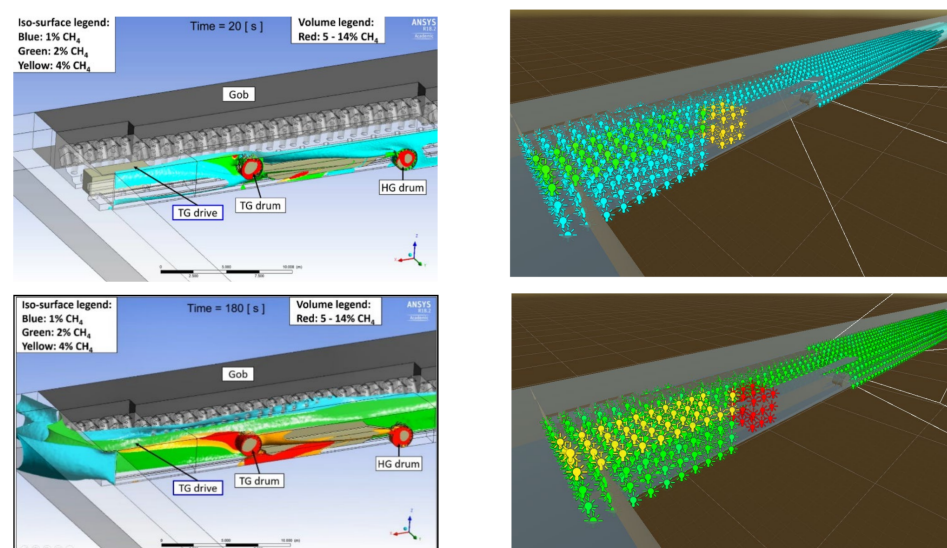


Figure 6. Side-by-side comparisons of CFD models and prediction visualizations modid.

These visualizations will help us conduct a user study with the aim of discovering a better way to visualize AI outcomes. The user study will also provide insights regarding the possible integration of these visualizations into a mixed-reality environment.

Author Contributions: Conceptualization, H.S.D., J.B. and G.B.; data curation, D.C.D. and A.J.; formal analysis, D.C.D.; funding acquisition, J.B.; investigation, D.C.D.; methodology, D.C.D. and H.S.D.; project administration, H.S.D., J.B. and G.B.; software, D.C.D. and A.J.; supervision, H.S.D., A.J., J.B. and G.B.; validation, D.C.D.; visualization, D.C.D.; writing—original draft, D.C.D.; writing—review and editing, H.S.D. and A.J. All authors have read and agreed to the published version of the manuscript.

Funding: This study was supported by the National Institute for Occupational Safety and Health (NIOSH), grant number 0000HCCR-2019-36403.

Institutional Review Board Statement: The study did not require ethical approval.

Informed Consent Statement: The study did not involve humans.

Data Availability Statement: Data presented in this study are available on request from the corresponding author. On account of their large size (12 TB), data are not publicly available due to online data storage requirements and associated long-term maintenance costs. Data presented in this study were not previously used or published. Data contained in this study were not altered, modified, or changed using any means. Data were exported from a CFD model that simulates an actual working mine.

Acknowledgments: This study utilized resources from Colorado School of Mines' CyberInfrastructure and Advanced Research Computing (CIARC) team and the University of Colorado Boulder Research Computing Group, which is supported by the National Science Foundation (awards ACI-1532235 and ACI-1532236), the University of Colorado, Boulder, and Colorado State University RMACC Summit.

Conflicts of Interest: The authors declare no conflict of interest. The funders had no role in the design of the study; in the collection, analyses, or interpretation of data; in the writing of the manuscript; or in the decision to publish the results.

References

1. Dudley, B. BP Statistical Review of World Energy. *BP Stat. Rev. Lond. UK* Accessed Aug. **2018**, *6*, 116.
2. Peng, S.S. *Longwall Mining*; CRC Press: Boca Raton, FL, USA, 2019; ISBN 9780429260049.
3. Qiao, M.; Ren, T.; Roberts, J.; Yang, X.; Li, Z.; Wu, J. New Insight into Proactive Goaf Inertisation for Spontaneous Combustion Management and Control. *Process Saf. Environ. Prot.* **2022**, *161*, 739–757. [[CrossRef](#)]
4. Juganda, A. *Evaluation of Point-Based Methane Monitoring and Proximity Detection for Methane Explosive Zones in Longwall Faces of Underground Coal Mines*; Colorado School of Mines: Golden, CO, USA, 2020.
5. Juganda, A.; Strebinger, C.; Brune, J.F.; Bogin, G.E. Discrete Modeling of a Longwall Coal Mine Gob for CFD Simulation. *Int. J. Min. Sci. Technol.* **2020**, *30*, 463–469. [[CrossRef](#)]
6. Davis, S.G.; Engel, D.; van Wingerden, K. Complex Explosion Development in Mines: Case Study—2010 Upper Big Branch Mine Explosion. *Process Saf. Prog.* **2015**, *34*, 286–303. [[CrossRef](#)]
7. Demirkan, D.C.; Duzgun, S.; Juganda, A.; Brune, J.; Bogin, G. Evaluation of Time Series Artificial Intelligence Models for Real-Time/near-Real-Time Methane Prediction in Coal Mines. *CIM J.* **2022**, *1*, 1–10. [[CrossRef](#)]
8. Karacan, C.Ö. Modeling and Prediction of Ventilation Methane Emissions of U.S. Longwall Mines Using Supervised Artificial Neural Networks. *Int. J. Coal. Geol.* **2008**, *73*, 371–387. [[CrossRef](#)]
9. Dougherty, H.N.; Özgen Karacan, C. A New Methane Control and Prediction Software Suite for Longwall Mines. *Comput. Geosci.* **2011**, *37*, 1490–1500. [[CrossRef](#)]
10. Duda, A.; Krzemień, A. Forecast of Methane Emission from Closed Underground Coal Mines Exploited by Longwall Mining—A Case Study of Anna Coal Mine. *J. Sustain. Min.* **2018**, *17*, 184–194. [[CrossRef](#)]
11. Sidorenko, A.A.; Dmitriev, P.N.; Sirenko, Y.G. Predicting Methane Emissions from Multiple Gas-Bearing Coal Seams to Longwall Goafs at Russian Mines. *ARPN J. Eng. Appl. Sci.* **2021**, *16*, 851–857.
12. Chen, P.-H.C.; Gadepalli, K.; MacDonald, R.; Liu, Y.; Kadowaki, S.; Nagpal, K.; Kohlberger, T.; Dean, J.; Corrado, G.S.; Hipp, J.D.; et al. An Augmented Reality Microscope with Real-Time Artificial Intelligence Integration for Cancer Diagnosis. *Nat. Med.* **2019**, *25*, 1453–1457. [[CrossRef](#)]
13. Nyanteh, Y.; Edrington, C.; Srivastava, S.; Cartes, D. Application of Artificial Intelligence to Real-Time Fault Detection in Permanent-Magnet Synchronous Machines. *IEEE Trans. Ind. Appl.* **2013**, *49*, 1205–1214. [[CrossRef](#)]

14. McGovern, A.; Elmore, K.L.; Gagne, D.J.; Haupt, S.E.; Karstens, C.D.; Lagerquist, R.; Smith, T.; Williams, J.K. Using Artificial Intelligence to Improve Real-Time Decision-Making for High-Impact Weather. *Bull. Am. Meteorol. Soc.* **2017**, *98*, 2073–2090. [[CrossRef](#)]
15. Imran, M.; Castillo, C.; Lucas, J.; Meier, P.; Vieweg, S. AIDR: Artificial Intelligence for Disaster Response. In Proceedings of the 23rd International Conference on World Wide Web, Seoul, Korea, 7–11 April 2014; Volume 1, pp. 159–162. [[CrossRef](#)]
16. Dong, M.; Wu, H.; Hu, H.; Azzam, R.; Zhang, L.; Zheng, Z.; Gong, X. Deformation Prediction of Unstable Slopes Based on Real-Time Monitoring and Deepar Model. *Sensors* **2021**, *21*, 14. [[CrossRef](#)] [[PubMed](#)]
17. Rodríguez-Rangel, H.; Morales-Rosales, L.A.; Imperial-Rojo, R.; Roman-Garay, M.A.; Peralta-Peñuñuri, G.E.; Lobato-Báez, M. Analysis of Statistical and Artificial Intelligence Algorithms for Real-Time Speed Estimation Based on Vehicle Detection with YOLO. *Appl. Sci.* **2022**, *12*, 2907. [[CrossRef](#)]
18. Wahyono; Harjoko, A.; Dharmawan, A.; Adhinata, F.D.; Kosala, G.; Jo, K.H. Real-Time Forest Fire Detection Framework Based on Artificial Intelligence Using Color Probability Model and Motion Feature Analysis. *Fire* **2022**, *5*, 23. [[CrossRef](#)]
19. Bagnall, A.; Lines, J.; Bostrom, A.; Large, J.; Keogh, E. The Great Time Series Classification Bake off: A Review and Experimental Evaluation of Recent Algorithmic Advances. *Data Min. Knowl. Discov.* **2017**, *31*, 606–660. [[CrossRef](#)]
20. Lines, J.; Taylor, S.; Bagnall, A. Time Series Classification with HIVE-COTE: The Hierarchical Vote Collective of Transformation-Based Ensembles. *ACM Trans. Knowl. Discov. Data* **2018**, *12*, 1. [[CrossRef](#)]
21. Dempster, A.; Petitjean, F.; Webb, G.I. ROCKET: Exceptionally Fast and Accurate Time Series Classification Using Random Convolutional Kernels. *Data Min. Knowl. Discov.* **2020**, *34*, 1454–1495. [[CrossRef](#)]
22. Shifaz, A.; Pelletier, C.; Petitjean, F.; Webb, G.I. *TS-CHIEF: A Scalable and Accurate Forest Algorithm for Time Series Classification*; Springer: Berlin, Germany, 2020; Volume 34, ISBN 1061802000.
23. Ismail Fawaz, H.; Lucas, B.; Forestier, G.; Pelletier, C.; Schmidt, D.F.; Weber, J.; Webb, G.I.; Idoumghar, L.; Muller, P.A.; Petitjean, F. InceptionTime: Finding AlexNet for Time Series Classification. *Data Min. Knowl. Discov.* **2020**, *34*, 1936–1962. [[CrossRef](#)]
24. He, K.; Zhang, X.; Ren, S.; Sun, J. Deep Residual Learning for Image Recognition. *Proc. IEEE Comput. Soc. Conf. Comput. Vis. Pattern Recognit.* **2016**, *2016*, 770–778. [[CrossRef](#)]
25. Schäfer, P.; Leser, U. Fast and Accurate Time Series Classification with WEASEL. In Proceedings of the 2017 ACM on Conference on Information and Knowledge Management, Singapore, 6–10 November 2017; Association for Computing Machinery: New York, NY, USA, 2017; pp. 637–646.
26. Lucas, B.; Shifaz, A.; Pelletier, C.; O’Neill, L.; Zaidi, N.; Goethals, B.; Petitjean, F.; Webb, G.I. Proximity Forest: An Effective and Scalable Distance-Based Classifier for Time Series. *Data Min. Knowl. Discov.* **2019**, *33*, 607–635. [[CrossRef](#)]
27. Deng, H.; Runger, G.; Tuv, E.; Vladimir, M. A Time Series Forest for Classification and Feature Extraction. *Inf. Sci.* **2013**, *239*, 142–153. [[CrossRef](#)]
28. Li, K.; Principe, J.C. Transfer Learning in Adaptive Filters: The Nearest Instance Centroid-Estimation Kernel Least-Mean-Square Algorithm. *IEEE Trans. Signal Process.* **2017**, *65*, 6520–6535. [[CrossRef](#)]
29. Alléon, A.; Jauvion, G.; Quennehen, B.; Lissmyr, D. PlumeNet: Large-Scale Air Quality Forecasting Using a Convolutional LSTM Network. *arXiv* **2020**, arXiv:2006.09204. Available online: <https://arxiv.org/pdf/2006.09204.pdf> (accessed on 3 May 2022).
30. Marts, J.A.; Gilmore, R.C.; Brune, J.F.; Bogin, G.E.; Grubb, J.W.; Saki, S. Dynamic Gob Response and Reservoir Properties for Active Longwall Coal Mines. *Min. Eng.* **2014**, *66*, 41–48.
31. Krickovic, S.; Findlay, C. Methane Emission Rate Studies in a Central Pennsylvania Mine. U S Bur Mines, Rep Invest 7591. 1971. Available online: <https://www.cdc.gov/NIOSH/mining/UserFiles/works/pdfs/ri7591.pdf> (accessed on 29 August 2022).
32. Peng, S.S.; Chiang, H.S. Air Velocity Distribution Measurements on Four Mechanized Longwall Coal Faces. *Int. J. Min. Geol. Eng.* **1986**, *4*, 235–246. [[CrossRef](#)]
33. Schatzel, S.J.; Krog, R.B.; Dougherty, H. Methane Emissions and Airflow Patterns on a Longwall Face: Potential Influences from Longwall Gob Permeability Distributions on a Bleederless Longwall Panel. *Trans. Soc. Min. Met. Explor. Inc* **2017**, *342*, 51–61. [[CrossRef](#)]
34. Gangrade, V.; Schatzel, S.J.; Harteis, S.P.; Addis, J.D. Investigating the Impact of Caving on Longwall Mine Ventilation Using Scaled Physical Modeling. *Min Met. Explor.* **2019**, *36*, 729–740. [[CrossRef](#)]
35. Hyndman, R.J.; Athanasopoulos, G. *Forecasting: Principles and Practice*; OTexts: Heathmont, VIC, Australia, 2018; ISBN 0987507117.
36. Sak, H.; Senior, A.; Beaufays, F. Long Short-Term Memory Based Recurrent Neural Network Architectures for Large Vocabulary Speech Recognition. *arXiv* **2014**, arXiv:1402.1128. Available online: <https://arxiv.org/pdf/1402.1128.pdf> (accessed on 3 May 2022).
37. Olah, C. Understanding LSTM Networks. Available online: <https://colah.github.io/posts/2015-08-Understanding-LSTMs/#fn1> (accessed on 6 September 2022).
38. Ismail Fawaz, H.; Forestier, G.; Weber, J.; Idoumghar, L.; Muller, P.A. Deep Learning for Time Series Classification: A Review. *Data Min. Knowl. Discov.* **2019**, *33*, 917–963. [[CrossRef](#)]
39. Graves, A.; Liwicki, M.; Fernández, S.; Bertolami, R.; Bunke, H.; Schmidhuber, J. A Novel Connectionist System for Unconstrained Handwriting Recognition. *IEEE Trans. Pattern Anal. Mach. Intell.* **2009**, *31*, 855–868. [[CrossRef](#)] [[PubMed](#)]
40. Greff, K.; Srivastava, R.K.; Koutnik, J.; Steunebrink, B.R.; Schmidhuber, J. LSTM: A Search Space Odyssey. *IEEE Trans. Neural Networks Learn. Syst.* **2017**, *28*, 2222–2232. [[CrossRef](#)] [[PubMed](#)]

41. Calin, O. *Recurrent Neural Networks B-Deep Learning Architectures: A Mathematical Approach*; Calin, O., Ed.; Springer International Publishing: Cham, Switzerland, 2020; pp. 543–559; ISBN 978-3-030-36721-3.
42. Hochreiter, S.; Schmidhuber, J. Long Short-Term Memory. *Neural. Comput.* **1997**, *9*, 1735–1780. [[CrossRef](#)]
43. Bengio, Y. Learning Long-Term Dependencies with Gradient Descent Is Difficult. *IEEE Trans. Neural Netw.* **1994**, *5*, 157–167. [[CrossRef](#)]
44. Gholamy, A.; Kreinovich, V.; Kosheleva, O. Why 70/30 or 80/20 Relation Between Training and Testing Sets: A Pedagogical Explanation. *Dep. Tech. Rep.* **2018**, *1*, 1–6.
45. Gholami, V.; Torkaman, J.; Dalir, P. Simulation of Precipitation Time Series Using Tree-Rings, Earlywood Vessel Features, and Artificial Neural Network. *Theor. Appl. Climatol.* **2019**, *137*, 1939–1948. [[CrossRef](#)]
46. Dubbs, A. Test Set Sizing Via Random Matrix Theory. *arXiv* **2021**, arXiv:2112.05977. Available online: <https://arxiv.org/pdf/2112.05977.pdf> (accessed on 29 August 2022).
47. Joseph, V.R. Optimal Ratio for Data Splitting. *Stat. Anal. Data Min.* **2022**, 531–538. [[CrossRef](#)]
48. Guyon, I. A Scaling Law for the Validation-Set Training-Set Size Ratio. *ATT Bell Lab.* **1997**, *1*, 1–11.